10-2001

Theoretical study of spin-orbit coupling constants for O+2 (A 2Π3/2,1/2u, v+=0–17 and a 4Π5/2,3/2,1/2,–1/2u, v+=0–25)

Dmitri G. Fedorov
Iowa State University

Mark S. Gordon
Iowa State University, mgordon@iastate.edu

Y. Song
Iowa State University

C. Y. Ng
Iowa State University

Theoretical study of spin-orbit coupling constants for O+2 (A 2Π3/2,1/2u, v+=0–17 and a 4Π5/2,3/2,1/2,–1/2u, v+=0–25)

Abstract
The spin-orbit coupling constants (Av+) for O+2(A 2Πu,v+=0–17) and O+2(a 4Πu,v+=0–25) were computed based on the Pauli–Breit Hamiltonian with one and two electron terms for comparison with experimental measurements. In the present theoretical study, the vibrational wave functions are obtained using the potential energy curve calculated at the multireference configuration interaction (MRCI) level of theory, with single and double excitations from the complete active space self-consistent field (CASSCF) reference wave function. The electronic wave functions and spin-orbit coupling constants are obtained at the CASSCF and restricted MRCI levels. The effect on Av+ for O+2(A 2Πu,v+) and O+2(a 4Πu,v+) due to interactions of the O+2(A 2Πu,v+), O+2(a 4Πu,v+), and O+2(2Σ+u)states is examined. The theoretical Av+ predictions for O+2(A 2Πu,v+) are found to be consistent with the experimental finding that O+2(A 2Πu) is an inverted spin-orbit state at low v+ levels and becomes a regular spin-orbit state at higher v+ levels. Good accord between theoretical predictions and experimental results for O+2(A 2Πu,v+=0–12) is observed with discrepancies in the range of 2–10 cm^{-1}. In the case of O+2(a 4Πu,v+), excellent agreement between theoretical *ab initio* and experimental results is found with a discrepancy of 2–5 cm^{-1}. Our effort to theoretically reproduce experimental fine structure in the Av+ curve for O+2(a 4Πu,v+) based on interstate vibrational interactions has met with limited success.

Keywords
Spin orbit interactions, Wave functions, Ab initio calculations, Configuration interaction, Excited states

Disciplines
Chemistry

Comments
The following article appeared in *Journal of Chemical Physics* 115 (2001): 7393, and may be found at doi:10.1063/1.1402170.

Theoretical study of spin-orbit coupling constants for O 2 + (A 2 Π 3/2,1/2u , v + =0–17 and a 4 Π 5/2,3/2,1/2,−1/2u , v + =0–25)

D. G. Fedorov, M. S. Gordon, Y. Song, and C. Y. Ng

Citation: The Journal of Chemical Physics **115**, 7393 (2001); doi: 10.1063/1.1402170
View online: http://dx.doi.org/10.1063/1.1402170
View Table of Contents: http://scitation.aip.org/content/aip/journal/jcp/115/16?ver=pdfcov
Published by the AIP Publishing

Theoretical study of spin-orbit coupling constants for O_2^+ ($A\,^2\Pi_{3/2,1/2u}$, $v^+=0-17$ and $a\,^4\Pi_{5/2,3/2,1/2,-1/2u}$, $v^+=0-25$)

D. G. Fedorov, M. S. Gordon, Y. Song, and C. Y. Ng
Ames Laboratory, United States Department of Energy and Department of Chemistry, Iowa State University, Ames, Iowa 50011

(Received 19 December 2000; accepted 20 July 2001)

The spin-orbit coupling constants (A_{v^+}) for $O_2^+(A\,^2\Pi_u, v^+=0-17)$ and $O_2^+(a\,^4\Pi_u, v^+=0-25)$ were computed based on the Pauli–Breit Hamiltonian with one and two electron terms for comparison with experimental measurements. In the present theoretical study, the vibrational wave functions are obtained using the potential energy curve calculated at the multireference configuration interaction (MRCI) level of theory, with single and double excitations from the complete active space self-consistent field (CASSCF) reference wave function. The electronic wave functions and spin-orbit coupling constants are obtained at the CASSCF and restricted MRCI levels. The effect on A_{v^+} for $O_2^+(A\,^2\Pi_u, v^+)$ and $O_2^+(a\,^4\Pi_u, v^+)$ due to interactions of the $O_2^+(A\,^2\Pi_u, v^+)$, $O_2^+(a\,^4\Pi_u, v^+)$, and $O_2^+(^2\Sigma_u^+)$ states is examined. The theoretical A_{v^+} predictions for $O_2^+(A\,^2\Pi_u, v^+)$ are found to be consistent with the experimental finding that $O_2^+(A\,^2\Pi_u)$ is an inverted spin-orbit state at low v^+ levels and becomes a regular spin-orbit state at higher v^+ levels. Good accord between theoretical predictions and experimental results for $O_2^+(A\,^2\Pi_u, v^+=0-12)$ is observed with discrepancies in the range of 2–10 cm^{-1}. In the case of $O_2^+(a\,^4\Pi_u, v^+)$, excellent agreement between theoretical *ab initio* and experimental results is found with a discrepancy of 2–5 cm^{-1}. Our effort to theoretically reproduce experimental fine structure in the A_{v^+} curve for $O_2^+(a\,^4\Pi_u, v^+)$ based on interstate vibrational interactions has met with limited success. © *2001 American Institute of Physics.* [DOI: 10.1063/1.1402170]

I. INTRODUCTION

Considerable uncertainty has existed concerning the interpretation of the spin-orbit coupling in the $O_2^+(A\,^2\Pi_u)$ state.[1–6] On the basis of a previous $O_2^+(A\,^2\Pi_u) \rightarrow O_2^+(X\,^2\Pi_g)$ emission study, Stevens concluded that low v^+ vibrational levels for $O_2^+(A\,^2\Pi_u)$ were regular and have positive spin-orbit coupling constants A_{v^+}.[1,2] However, the subsequent analysis of new emission bands showed that A_{v^+} is negative, i.e., inverted, for $v^+=0$, 5, and 6 and positive for $v^+=8$, providing the first evidence that the $O_2^+(A\,^2\Pi_u)$ state changes from an inverted state to a regular state around $v^+=7$.[3] This conclusion was supported by the critical analysis of early emission data by Albritton *et al.*[4] The high-resolution emission experiment of Coxon and Haley[5] has provided the most precise spectroscopic constants for O_2^+ ($A\,^2\Pi_u$; $v^+=0-8$ and 11–15). The A_{v^+} values derived are consistent with the trend suggested by Albritton *et al.* The latter experiment also revealed anomalous behavior for most of the spectroscopic constants for high v^+ levels of the $O_2^+(A\,^2\Pi_u)$ state. Discontinuities observed for the v^+-dependencies of the Λ-doubling, centrifugal distortion, and spin-rotation constants strongly suggest the presence of a perturbation state near $v^+=9$. Referring to previous *ab initio* calculations,[7,8] Coxon and Haley suggested that the shallow-bound $^2\Sigma_u^+$ state correlating with the $O^+(^4S)+O(^3P)$ dissociation limit is the likely perturbing state.

Reliable calculations on spin-orbit interactions have not been readily accessible due to the requirement of accurate electronic and vibrational wave functions. To our knowledge, the only previous theoretical investigation on the vibrational dependence of the spin-orbit coupling constant for O_2^+ was made by Raftery and Richards.[6] While the agreement between theoretical predictions and experimental observations for O_2^+ ($X\,^2\Pi_g$ and $a\,^4\Pi_u$; v^+) was reasonable, the theoretical A_{v^+} predictions for $O_2^+(A\,^2\Pi_u; v^+)$ compare poorly with experimental results, possibly owing to the neglect of two-center integrals and the inadequacy of the wave functions employed. By employing an empirical correction, they arrived at a set of positive A_{v^+} values for $O_2^+(A\,^2\Pi_u; v^+)$, showing the regular downward trend in the A_{v^+} values with increasing v^+. In view of the small A_v^+ values for $O_2^+(A\,^2\Pi_u; v^+)$, reliable predictions would require a higher level *ab initio* study.

Using a synchrotron-based pulsed-field ionization-photoelectron (PFI-PE) method, we have recently obtained reliable A_{v^+} values for several diatomic ions in the ground and excited electronic states with v^+ close to their dissociation limits, such as $O_2^+(X\,^2\Pi_g, v^+=0-38)$,[9] $O_2^+(a\,^4\Pi_u, v^+=0-18)$,[10] and $CO^+(A\,^2\Pi; v^+=0-41)$.[11] Since the A_{v^+} values for $O_2^+(A\,^2\Pi_u, v^+=0-12)$[12] are close to the PFI-PE energy resolution, accurate A_{v^+} values cannot be obtained by simulation of the PFI-PE bands. However, the simulation supports the conclusion of the previous emission study[5] that the O_2^+ ($A\,^2\Pi_u$, $v^+=9$ and 10) states are strongly perturbed by a nearby electronic state. The PFI-PE data also provide evidence that $|A_v^+| \leqslant 6\ cm^{-1}$ for $O_2^+(A\,^2\Pi_{3/2,1/2u}, v^+=0-12)$ and that the simulation prefers negative A_v^+ values at low v^+.[12] The PFI-PE studies helped to stimulate the development of a new *ab initio* computational code[11] for calculating A_{v^+} values associated with a

wide range of vibrational energy levels. The code included in the publicly available quantum chemistry package GAMESS[13] has the capability of performing efficient spin-orbit coupling calculations for arbitrary spin multiplicities with any configuration interaction (CI) wave-function types supported by GAMESS, for both one and two electron spin-orbit coupling operators.[11] Using this new capability, we have previously calculated A_{v^+} values for $CO^+(A\,^2\Pi_{3/2,1/2}, v^+=0-41)$ and $O_2^+(X\,^2\Pi_{1/2,3/2g}, v^+=0-38)$, which are found to be in good accord with experimental PFI-PE measurements.[11] In this article, we present results of a similar theoretical study on the spin-orbit coupling interactions for $O_2^+(A\,^2\Pi_u, v^+=0-17)$ and $O_2^+(a\,^4\Pi_u, v^+=0-25)$. The nature of the perturbation by the $^2\Sigma_u^+$ state,[5] which correlates with the $O^+(^4S)+O(^3P)$ dissociation limit, is also examined.

II. THEORETICAL METHODS

A. Energy levels and spin-orbit coupling

The method used to calculate *ab initio* A_{v^+} values is described in greater detail in Ref. 11. All calculations were performed with a fairly large basis set (the AVTZ basis in MOLPRO).[14–18] The potential energy curve for O_2^+ as a function of the O–O distance (R) was determined (using MOLPRO) at the multireference configuration interaction (MRCI) level of theory, with single and double (SD) excitations from the complete active space self-consistent field (CASSCF)[19] reference wave function. The full valence active space includes 11 electrons in 8 orbitals ($2s$ and $2p$).[13] The core $1s$ orbitals were correlated at the CI step with single and double excitations into the virtual space. This method is denoted as MR(SD)CI.

The spin-orbit coupling matrix elements as a function of R were calculated separately for each pair of electronic states with GAMESS,[13] using the full Breit–Pauli Hamiltonian[20] with both CASSCF and truncated second-order configuration interaction (SOCI) levels of theory. The SOCI wave function differs from the MR(SD)CI wave function that was used to obtain the energy. The MR(SD)CI wave function takes into consideration all contracted single and double excitations from the CASSCF space into the full virtual space (82 orbitals), whereas the SOCI virtual space is limited to 26 orbitals. In addition, the SOCI wave function includes no core excitations. The size of the SOCI virtual space was chosen to maintain a manageable number of configuration state functions (between 200 000 and 300 000). The cutoff to limit the virtual space was determined by choosing all low-lying virtual orbitals that are separated from the rest of the virtual space by an energy gap of 0.4133 and 1.0504 hartree at equilibrium and dissociation limit, correspondingly. In addition, molecular orbitals were separately optimized for each state at the MR(SD)CI level, and a single set of orbitals was optimized for the $A\,^2\Pi_u$ state and subsequently used for all states at the SOCI level. The first-order CI (FOCI) method was also explored, in which all uncontracted single excitations from the CASSCF space into the full virtual space of 82 orbitals are included. However, the spin-orbit coupling constants predicted by this level of theory are unacceptably poor as compared to the experimental results, so this method was not extensively pursued. All calculations were performed in the Abelian subgroup of $D_{\infty h}(D_{2h})$.

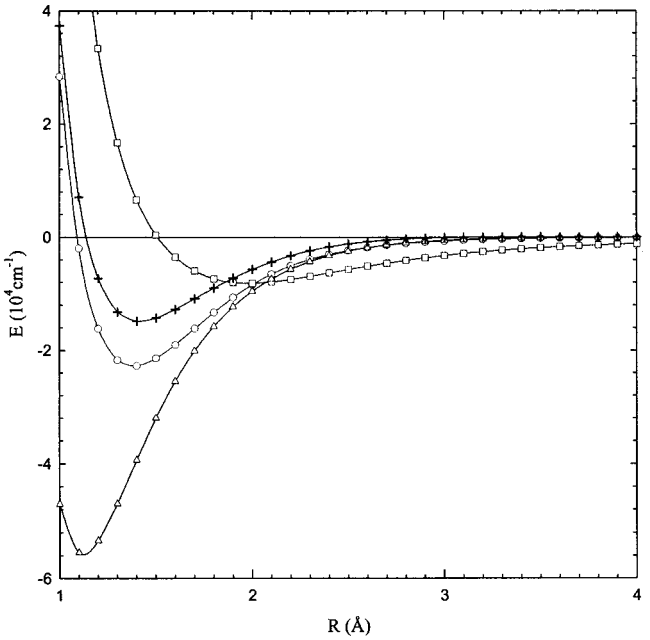

FIG. 1. Potential energy curves for $O_2^+(X\,^2\Pi_g)$ (△), $O_2^+(A\,^2\Pi_u)$ (○), $O_2^+(a\,^4\Pi_u)$ (+), and $O_2^+(^2\Sigma_u^+)$ (□) calculated at the MR(SD)CI level.

The potential energy curves for O_2^+ ($X\,^2\Pi_g$, $A\,^2\Pi_u$, $a\,^4\Pi_u$, and $^2\Sigma_u^+$) calculated at the MR(SD)CI level are shown in Fig. 1, while the potential energy curves for $O_2^+(A\,^2\Pi_u$, $a\,^4\Pi_u$, and $^2\Sigma_u^+)$ obtained using the SOCI method are presented in Fig. 2. The behavior of the two sets of curves is clearly similar.

As in previous calculations, the eigenfunctions of the Morse potential[21]

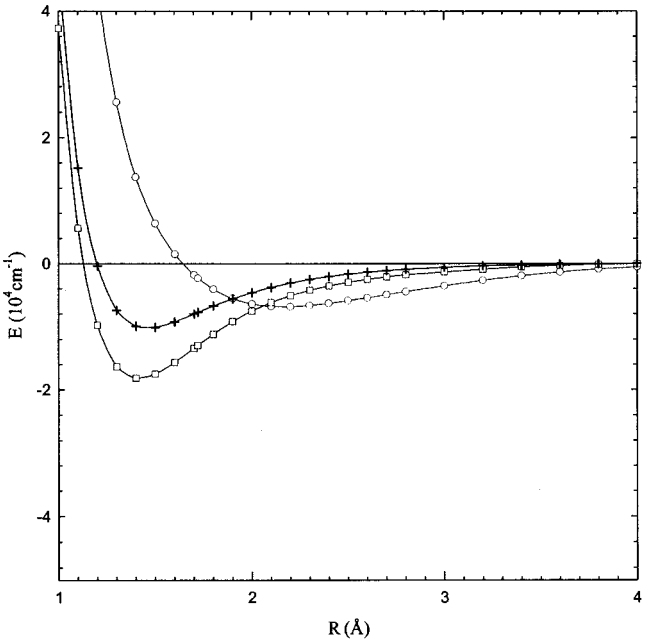

FIG. 2. Potential energy curves for $O_2^+(A\,^2\Pi_u)$ (□), $O_2^+(a\,^4\Pi_u)$ (+), and $O_2^+(^2\Sigma_u^+)$ (○) calculated at the SOCI level.

TABLE I. Parameters[a] for the Morse potential $[U(R)=D_e\{1-\exp[-\alpha(R-R_e)]\}^2,]$ for $O_2^+(A\,^2\Pi_u)$ obtained by fitting the *ab initio* potential energies.

Morse Potential	R_e (Å)	a (Å^{-1})	D_e (cm^{-1})	ω_e^+ (cm^{-1})	$\omega_e^+\chi_e^+$ (cm^{-1})
Expt. $O_2^+(A\,^2\Pi_u)$[b,c]	1.4090	2.5376	14 864.7	898.25(898.10)	13.57(13.22)
Theor. $O_2^+(A\,^2\Pi_u)$[d]	1.410	2.5607	15 096.1	913.44	13.82
Theor. $O_2^+(A\,^2\Pi_u)$[e]	1.45	2.675	10 533.	797.1	15.1
Expt. $O_2^+(a\,^4\Pi_u)$[b,c]	1.3813	2.2205	25 809.9	1035.69(1035.9)	10.39(10.20)
Theor. $O_2^+(a\,^4\Pi_u)$[d]	1.372	2.4582	22 904.4	1080.09	12.73
Theor. $O_2^+(a\,^4\Pi_u)$[e]	1.42	2.399	18 203.8	939.7	12.1
Theor. $O_2^+(^2\Sigma_u^+)$[d]	1.97 0	1.5554	7605.6	393.83	5.10
Theor. $O_2^+(^2\Sigma_u^+)$[e]	2.18	1.296	7029.0	315.4	3.5

[a]R_e is the equilibrium bond distance for $O_2^+(A\,^2\Pi, v^+=0)$ and D_e = well depth, ω_e^+ = vibrational frequency, and $\omega_e^+\chi_e^+$ = anharmonicity for the Morse potential.
[b]Morse potential based on vibrational constants cited in Ref. 22.
[c]Values for ω_e^+ and $\omega_e^+\chi_e^+$ reported in Ref. 12 are given in parentheses.
[d]This work. Morse potential based on *ab initio* (MR(SD)CI) potential energies.
[e]This work. Morse potential based on *ab initio* (SOCI) potential energies.

$$[U(R)=D_e\{1-\exp[-a(R-R_e)]\}^2] \tag{1}$$

obtained by fitting the theoretical potential energy curves were used to calculate the nuclear wave functions.[11] The Morse parameters (R_e, a, and D_e) for the *ab initio* potentials obtained at the MR(SD)CI and SOCI levels of theory are compared in Table I with literature values[22] based on experimental measurements. As expected, the Morse potential fitted to the MR(SD)CI potential is in better agreement with the experimental values.

The *ab initio* spin-orbit coupling constant as a function of R, $A(R)$, was first calculated at discrete R values and then fitted to an appropriate analytic functional form for the convenience of performing numerical integration. The best fitted curve to $A(R)$ values was found to have the functional form

$$A(R)=h(1+\tanh(R-R_o)s)-A_0. \tag{2}$$

Table II summarizes the least square-fitted parameters h, R_o, s, and A_0 for the O_2^+ ($A\,^2\Pi_u$ and $a\,^4\Pi_u$) states calculated at the CASSCF and SOCI levels of theory. Here, h and A_0 are in cm^{-1}, R_o in Å, and s in Å^{-1}. The *ab initio* $A(R)$ values calculated using the CASSCF (solid dots) and SOCI (solid triangles) methods, together with their best-fitted curves (solid lines), are plotted in Fig. 3.

In order to gain a better understanding of the nature of the inversion of the spin-orbit coupling constant for $O_2^+(A\,^2\Pi_u)$, the one-electron and two-electron contributions to $A(R)$ were separately studied at the SOCI level. The one-electron contributions (open circles) and two-electron contributions (open squares), along with their sums (+), thus obtained for the R range of 1.0–4.0 Å are depicted in Fig. 4.

TABLE II. Parameters for the function $A(R)=h(1+\tanh[(R-R_o)s])-A_0$, which yield the best fit to the *ab initio* spin-orbit coupling constant calculated as a function of R.

Level of theory/states	h (cm^{-1})	R_o (Å)	s (Å^{-1})	A_0 (cm^{-1})
CASSCF/$O_2^+(A\,^2\Pi_u)$	37.0077	1.966 59	1.516 36	16.6459
CASSCF/$O_2^+(a\,^4\Pi_u)$	−14.7546	2.195 17	2.982 45	−21.2267
SOCI/$O_2^+(A\,^2\Pi_u)$	30.2944	1.970 05	1.817 22	17.9773
SOCI/$O_2^+(a\,^4\Pi_u)$	−14.1221	2.050 97	2.855 33	−22.9843

The detailed structure of the energies computed at the SOCI level near the crossing between the $O_2^+(A\,^2\Pi_u)$ and $O_2^+(^2\Sigma_u^+)$ states is shown in Fig. 5. In this figure, we show the weight of the adiabatic state $O_2^+(A\,^2\Pi_u)$ in the diabatic states ($\Omega=1/2$ and $\Omega=3/2$, where Ω denotes the absolute value of the J_Z operator), coupled by spin-orbit interaction, near the region where the surface crossing occurs. It also shows the splitting of the diabatic surfaces near the crossing. The $\Omega=3/2$ state is a pure $A\,^2\Pi_u$ state, so that its weight is not shown and the two $\Omega=1/2$ states come from coupling of the $A\,^2\Pi_{1/2u}$ and $^2\Sigma_{1/2u}^+$ states. The diabatic surfaces are obtained from diagonalization of the spin-orbit coupling Hamiltonian in the basis of the three states $A\,^2\Pi_u$, $a\,^4\Pi_u$, and $^2\Sigma_u^+$. The $a\,^4\Pi_u$ state is well-separated from the other two and exerts only a weak influence on them.

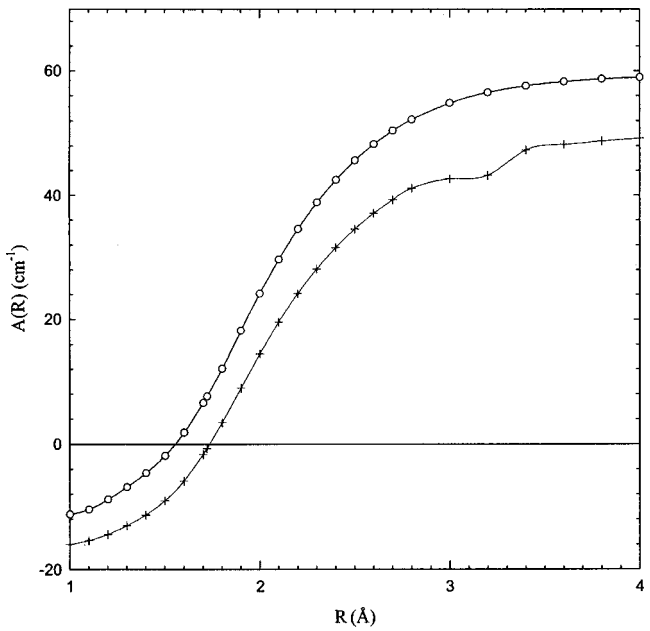

FIG. 3. The *ab initio* A(R) values for $O_2^+(A\,^2\Pi_u)$ calculated using the CASSCF (○) and SOCI (+) methods, together with the best-fitted curves (solid lines).

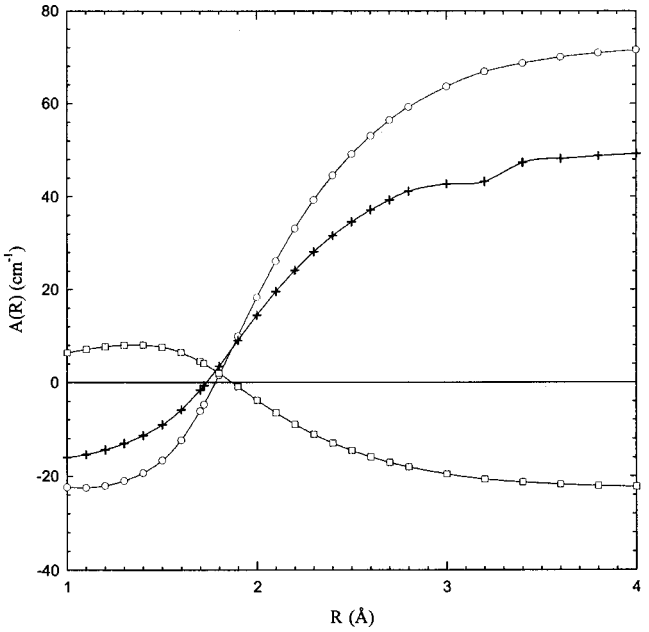

FIG. 4. The one-electron (○) and two-electron contributions (□) to the spin-orbit splitting constant (+) for $O_2^+(A\,^2\Pi_u)$, along with their sums (+) in the R range of 1.0–4.0 Å.

In order to better understand the discrepancy between theory and experiment, we also calculated A_{v^+} values based on computed vibrational wave functions obtained using the potential fitted to the experimental data, along with *ab initio* values of $A(R)$ based on the SOCI electronic wave function. This method is labeled the semiempirical-SOCI method here.

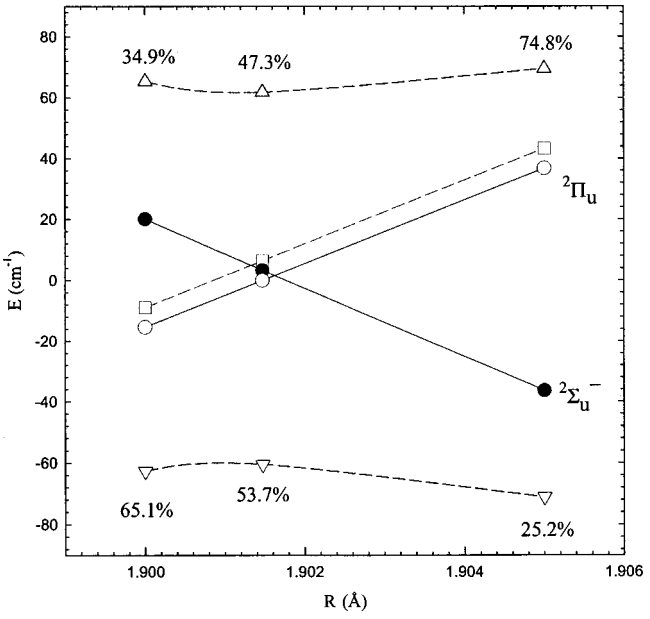

FIG. 5. The SOCI energies near the crossing between the $O_2^+(A\,^2\Pi_u)$ (○) and $O_2^+(^2\Sigma_u^-)$ (●) states (solid curves), showing the weight of the adiabatic $O_2^+(A\,^2\Pi_u)$ state in the diabatic representations [$\Omega=1/2$ (△ and ∇) and $\Omega=3/2$ (□)] (dashed curves), coupled by spin-orbit interaction.

B. Theoretical model for coupling of the vibrational states

In order to couple the vibrational states for particular electronic states, the following matrix is constructed and diagonalized (similarly to the scheme described in Ref. 23):

$$\langle \Psi_N^v \Psi_e^i | \hat{H} | \Psi_N^{v'} \Psi_e^{i'} \rangle, \tag{3}$$

where Ψ_N^v and Ψ_e^i are nuclear and electronic wave functions, respectively, for given combinations of vibrational (v) and electronic (i) states, and the scalar product is taken over both nuclear and electronic coordinates. The Hamiltonian operator can include any interactions of interest. For the purpose of this paper, it includes the usual nonrelativistic Hamiltonian and spin-orbit coupling operators. The number of states to be included depends on the desired accuracy of the results. The influence of a state (v',i') upon the state of primary interest (v,i) can be estimated by means of perturbation theory:

$$\frac{|\langle \Psi_N^v \Psi_e^i | \hat{V} | \Psi_N^{v'} \Psi_e^{i'} \rangle|^2}{E-E'}, \tag{4}$$

where V is the coupling potential (e.g., spin-orbit coupling) and E and E' are the energies of the (v,i) and (v',i') states, respectively.

For spin-orbit coupling in diatomic molecules, the matrix is block-diagonal for each eigenvalue (M_J) of the J_z operator. The eigenvalues of this matrix provide diabatic vibrational levels that include coupling between adiabatic states. For relatively weak coupling, the diabatic states retain discernable adiabatic character, and the effect of the coupling may be manifested experimentally as small bumps on the plots depicting the dependence of A_{v^+}'s upon the vibrational quantum number v^+.

For the system of interest, a single electronic state picture would produce a 4×4 (8×8) matrix for $O_2^+(A\,^2\Pi_u)$ $[O_2^+(a\,^4\Pi_u)]$ states. This matrix is block-diagonalized with 4 (8) blocks consisting of E_{MJ} values corresponding to $M_J = \pm1/2, \pm3/2, (\pm5/2, \pm3/2, \pm1/2, \mp1/2)$, with the property that the eigen-energy $E_{MJ}=E_{-MJ}$. The spin-orbit coupling constant can be easily calculated as, for example, $E_{1/2}-E_{3/2}$.

The three lowest excited O_2^+ states ($A\,^2\Pi_u$, $a\,^4\Pi_u$, and $^2\Sigma_u^+$) interacting by means of spin-orbit coupling in O_2^+ were coupled using this model. In the case of $O_2^+(a\,^4\Pi_u)$, accounting for the vibrational energies shifts the various M_J levels by different amounts. Consequently, the uniform splitting between all four distinct spin-orbit levels becomes nonuniform. In order to compare the theoretical predictions with the experiments, from which a single averaged spin-orbit splitting constant is reported for each multiplet, the shift in each $|M_J|$ level due to vibrational energies was added to the uniform constant with equal weight (1/4). It should be noted that at very large distances, additional states interact with $^2\Pi_u$, so that a quantitatively correct description of the spin-orbit coupling behavior at the dissociation limit requires inclusion of these (atom-like) states. However, the value of the spin-orbit coupling at these large distances has only a

very weak influence upon the spin-orbit coupling of the lower vibrational levels, due to a negligible density of the vibrational states in that region.

For O_2^+, the value of $|\langle \Psi_N^v \Psi_e^i | \hat{V} | \Psi_N^{v'} \Psi_e^{i'} \rangle|$ is typically found to be on the order of 1–10 cm^{-1}. The typical value of $E-E'$ is >500–1000 cm^{-1}, except for nearest neighbors. Thus, only one vibrational level was included in the matrix for each electronic state. This produced a 4×4 $M_J=1/2$ matrix (built upon $A\,^2\Pi_{1/2u}$, $^2\Sigma^+_{1/2u}$, $a\,^4\Pi_{1/2u}$, and $a\,^4\Pi_{-1/2u}$), a 2×2 $M_J=3/2$ matrix ($A\,^2\Pi_{3/2u}$, $a\,^4\Pi_{3/2u}$) and a 1×1 $M_J=5/2$ matrix ($a\,^4\Pi_{5/2u}$) with the following structure, $H^{(M_J)}$:

$$H^{(1/2)} = \begin{bmatrix} -D_{e1}+E_{v1}-A_1/2 & \langle {}^2\Pi_{ux}(v1,-\tfrac{1}{2})|\hat{H}_{so}|{}^2\Sigma_u^+(v2,\tfrac{1}{2})\rangle & i\langle {}^2\Pi_{ux}(v1,-\tfrac{1}{2})|\hat{H}_{so}|{}^4\Pi_{uy}(v3,-\tfrac{1}{2})\rangle & 0 \\ \text{c.c.} & -D_{e2}+E_{v2} & \langle {}^2\Sigma_u^+(v2,+\tfrac{1}{2})|\hat{H}_{so}|{}^4\Pi_{ux}(v3,-\tfrac{1}{2})\rangle & -\sqrt{3}H_{23}^{(1/2)} \\ \text{c.c.} & \text{c.c.} & -D_{e3}+E_{v3}-A_3/2 & 0 \\ \text{c.c.} & \text{c.c.} & \text{c.c.} & -D_{e3}+E_{v3}-3A_3/2 \end{bmatrix}, \tag{5a}$$

$$H^{(3/2)} = \begin{bmatrix} -D_{e1}+E_{v1}+A_1/2 & H_{13}^{(1/2)} \\ \text{c.c.} & -D_{e3}+E_{v3}+A_3/2 \end{bmatrix}, \tag{5b}$$

$$H^{(5/2)} = [-D_{e3}+E_{v3}+3A_3/2], \tag{5c}$$

where D_e is the dissociation energy, E_v is the vibrational level energy (given for a Morse potential by $E_v=\omega_e(v+\frac{1}{2})-\omega_e x_e(v+\frac{1}{2})^2$), A_1 and A_3 are single electronic state spin-orbit coupling constants for $O_2^+(A\,^2\Pi_u)$ and $O_2^+(a\,^4\Pi_u)$, respectively, and c.c. in H_{ij} refers to the complex conjugate of H_{ji} since the Hamiltonian matrices are Hermitian. The numbers given in parentheses beside the electronic states, such as $^2\Pi_u(v,M_S)$ are the values of the vibrational quantum numbers v and M_S. Thus, three additional matrix elements are needed for this model: $H_{12}^{(1/2)}$, $H_{13}^{(1/2)}$, and $H_{23}^{(1/2)}$. They were computed with SOCI wave functions in the same manner as the spin-orbit splitting constant calculations described in the previous section.

In order to reproduce the experimental results, the zero-order levels (the diagonal elements) must be as accurate as the perturbation, on the order of a few cm^{-1} for this system. It is difficult for current *ab initio* electronic structure theory to provide such accuracy, whereas it is possible experimentally. However, it should be possible to use experimental levels for the diagonal matrix elements and *ab initio* coupling terms (off-diagonal elements) in order to understand the nature of the fine features.[11]

III. RESULTS AND DISCUSSION

As shown in Fig. 4, the one-electron contributions to $A(R)$ calculated at the SOCI level of theory are negative at $R<1.78$ Å and become positive at larger R. On the contrary, the two-electron contributions are positive at small R (<1.87 Å) and become negative at larger R. Thus, the one-electron and two-electron contributions are both positive only in a narrow range of R in the vicinity of $R=1.80$ Å. The $A(R)$ value, which is the sum of the two contributions, is negative at $R<1.72$ Å and becomes positive at $R>1.72$ Å. This crossover distance of 1.72 Å roughly determines the v^+ level for $O_2^+(A\,^2\Pi_u)$ at which A_{v+} would change sign.

The theoretical A_{v+} ($v^+=0-25$) values for $O_2^+(A\,^2\Pi_u)$ obtained using the CASSCF, SOCI, semiempirical SOCI, and the vibrational level coupling schemes (described in Sec. II B), together with the experimental A_{v+} ($v^+=0-8$ and 11–15), are plotted as a function of v^+ in Fig. 6. These theoretical and experimental A_{v+} are also tabulated in Table III. The theoretical A_{v+} curves obtained at the CASSCF, SOCI, and semiempirical SOCI are nearly parallel to the experimental A_{v+} curve as shown in Fig. 6, although this correspondence becomes worse at larger v^+ states. Further-

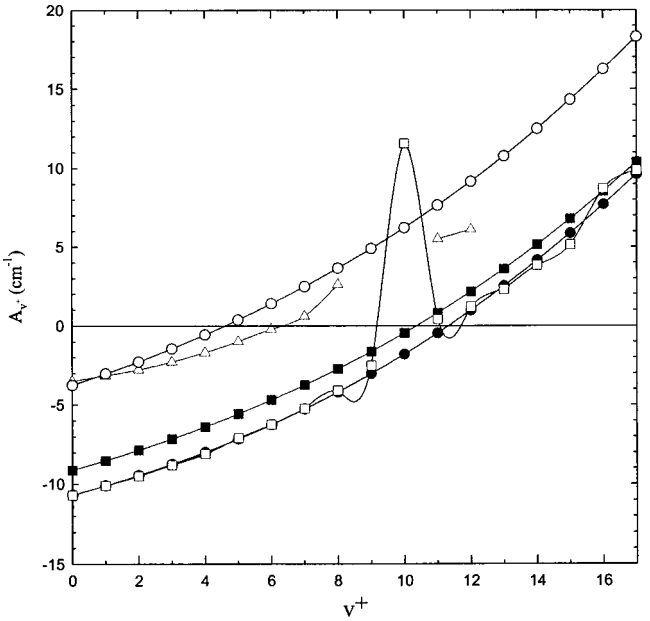

FIG. 6. Comparison between theoretical spin-orbit coupling constants (A_{v+},) for $O_2^+(A\,^2\Pi_u, v^+=0-17)$ computed using the CASSCF (○), SOCI (●), semiempirical SOCI (■), and vibrational level coupling (□) procedures and experimental A_{v+} ($v^+=0-12$) values (△) reported in Ref. 5.

TABLE III. Comparison of the experimental and theoretical spin-orbit constants A_{v^+} for $O_2^+(A\,^2\Pi_{3/2,1/2u}, v^+=0-17)$.

	Theoretical (cm^{-1})[a]				Experimental
v^+	CASSCF	SOCI	Vibrational	Semiempirical	(cm^{-1})[b]
0	−3.76	−10.69	−10.7	−9.13	−3.50
1	−3.04	−10.10	−10.1	−8.52	−3.16
2	−2.28	−9.46	−9.5	−7.86	−2.78
3	−1.45	−8.75	−8.8	−7.15	−2.28
4	−0.57	−7.99	−8.1	−6.39	−1.69
5	0.37	−7.15	−7.1	−5.57	−0.99
6	1.39	−6.25	−6.24	−4.69	−0.22
7	2.47	−5.26	−5.24	−3.74	0.6
8	3.64	−4.2	−4.1	−2.73	2.6
9	4.88	−3.04	−2.51	−1.63	
10	6.21	−1.8	11.57	−0.46	
11	7.64	−0.46	0.43	0.80	5.5
12	9.16	0.98	1.2	2.15	6.1
13	10.77	2.52	2.3	3.60	6.84
14	12.49	4.15	3.83	5.14	7.78
15	14.32	5.88	5.14	6.79	8.9
16	16.24	7.71	8.71	8.54	
17	18.28	9.62	9.88	10.40	

[a]This work.
[b]Reference 5.

TABLE IV. Comparison of the experimental and theoretical spin-orbit constants A_{v^+} for $O_2^+(a\,^4\Pi_{5/2,3/2,1/2,-1/2u}, v^+=0-25)$.

	Theoretical (cm^{-1})[a]				Experimental
v^+	CASSCF	SOCI	Vibrational	Semiempirical	(cm^{-1})[b]
0	49.85	46.44	46.44	46.41	48(47.79)
1	49.81	46.35	46.35	46.32	48(47.80)
2	49.77	46.25	46.25	46.21	48(47.77)
3	49.71	46.12	46.12	46.09	48(47.74)
4	49.65	45.98	45.98	45.95	48(47.71)
5	45.58	45.82	45.82	45.79	47(47.64)
6	49.49	45.64	45.64	45.61	48(47.55)
7	49.39	45.42	45.42	45.40	48(47.44)
8	49.28	45.18	45.18	45.17	48(47.06)
9	49.14	44.89	44.89	44.91	49(47.13)
10	48.97	44.57	44.57	44.61	46
11	48.78	44.20	44.20	44.28	47
12	48.54	43.78	43.78	43.91	51
13	48.27	43.30	43.30	43.49	43
14	47.95	42.77	42.75	43.03	47
15	47.56	42.17	42.13	42.52	47
16	47.11	41.50	41.44	41.96	43
17	46.58	40.76	40.66	41.35	46
18	45.97	39.96	39.69	40.69	45
19	45.26	39.10	38.74	39.99	
20	44.46	38.18	37.99	39.25	
21	43.55	37.22	38.21	38.46	
22	42.54	36.21	35.99	37.65	
23	41.45	35.18	35.11	36.82	
24	40.27	34.14	33.31	35.97	
25	39.03	33.09	33.02	35.11	

[a]This work.
[b]Reference 10. Values in parentheses are from Refs. 24 and 25.

more, all theoretical calculations predict that A_{v+} is negative at low v^+ states and becomes positive at higher v^+ states. The crossover v^+ state varies from $v^+=5$ at the CASSCF level to $v^+=12$ at the SOCI level. Thus, we may conclude that the theoretical calculations predict that the $O_2^+(A\,^2\Pi_u)$ state changes from a spin-orbit inverted state at low v^+ to a regular state around $v^+=5-12$. This prediction is in qualitative agreement with experimental findings. The inversion of A_{v+} for $O_2^+(A\,^2\Pi_u)$ is found to be caused by the mutual interaction of several states arising from the $(\sigma_g)^2(\pi_u)^3(\pi_g^*)^2$ configuration, as the contributing spin-orbit integrals between active orbitals come with opposite sign and weights determined by the CI coefficients, that change along the dissociation path. We note that the inversion occurs when the $A\,^2\Pi_u$ state is computed alone, so that the inversion phenomenon comes from this state itself. Certainly when the constant becomes very small, even weak influences by other states may cause a noticeable difference and slightly change the value of v^+ at which the inversion occurs.

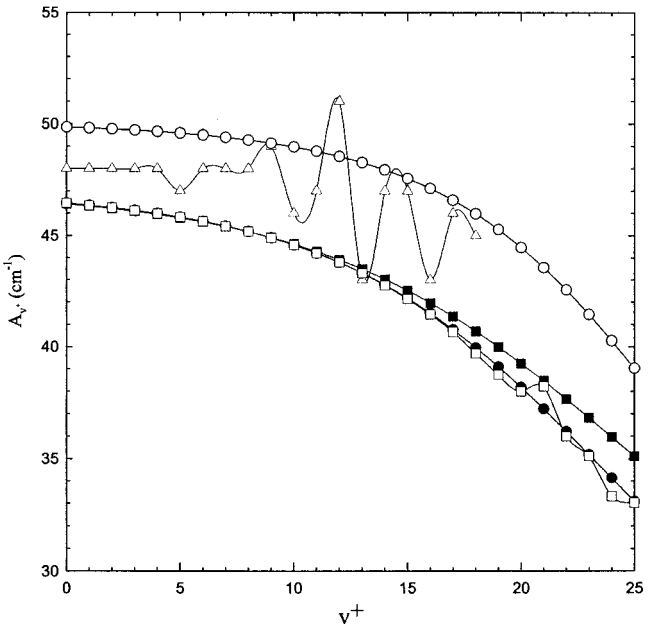

FIG. 7. The comparison between theoretical spin-orbit coupling constant (A_{v+}) for $O_2^+(a\,^4\Pi_u; v^+=0-25)$ computed using the CASSCF (○), SOCI (●), semiempirical SOCI (■), and vibrational level coupling (□) procedures and experimental A_{v+} ($v^+=0-18$) values (△) reported in Ref. 10.

The theoretical A_{v+} ($v^+=0-25$) values for $O_2^+(a\,^4\Pi_u)$ obtained at the CASSCF, SOCI, and multistate coupling level of theory, together with the experimental values[10,24,25] for A_{v+} ($v^+=0-18$), are depicted in Fig. 7. These theoretical and experimental[10,24,25] values are also listed in Table IV. The A_{v+} values calculated for $O_2^+(a\,^4\Pi_u)$ at the CASSCF level are higher than those at corresponding v^+ states obtained at the SOCI level by 3.5–6.0 cm^{-1}. Similar to the case of $O_2^+(A\,^2\Pi_u)$, the A_{v+} values calculated for $O_2^+(a\,^4\Pi_u)$ at the SOCI and semiempirical SOCI schemes are in good agreement, indicating that the use of the Morse potential fitted to experimental results in very little improvement over the *ab initio* potential. As shown in Fig. 7, the vibrational dependencies of the theoretical A_{v+} values for $O_2^+(a\,^4\Pi_u)$ are similar to the other levels of theory, showing a gradual decrease as v^+ is increased. The CASSCF A_{v+} values for $O_2^+(a\,^4\Pi_u)$ are generally higher than the corresponding experimental A_{v+} values,[10] while the SOCI values

for A_{v+} are generally lower than the corresponding experimental A_{v+} values. The average differences of 1–2 cm^{-1} between the *ab initio* and experimental A_{v+} values (excluding the fine features) are likely caused by neglected interactions, of which the most obvious candidate is the spin-spin coupling. Another important factor is the dynamic electron correlation, not fully accounted for since the virtual CI space was truncated in the SOCI calculations. A further possible factor is the deviation of the actual potential energy curve from that represented by the Morse potential, but this is probably a less important issue.

We observe that the much more expensive SOCI approach gives better values of spin-orbit coupling constants for larger v^+ (corresponding to larger internuclear separation) in case of $O_2^+(A\,^2\Pi_u)$, however CAS values are in better agreement with experiment for small v^+ in both $O_2^+(A\,^2\Pi_u)$ and $O_2^+(a\,^4\Pi_u)$. The lack of experimental data and very strong perturbations at large v^+ values leave some uncertainty with regard to whether CAS or SOCI values are better in that region in the case of $O_2^+(a\,^4\Pi_u)$. The truncation of the SOCI virtual space that we employed may have caused some numerical deterioration of the SOCI compared to the CAS approach.

Although the spin-orbit coupling of the electronic states $O_2^+(A\,^2\Pi_u)$ and $O_2^+(a\,^4\Pi_u)$ is very strong ($\approx$50–100 cm^{-1}), the spin-orbit couplings between vibrational levels of $O_2^+(A\,^2\Pi_u)$ and $O_2^+(a\,^4\Pi_u)$, are predicted to be small, typically less than $10^{-3}\,cm^{-1}$. These small spin-orbit interactions are attributed to the fact that the vibrational states of the two electronic states are centered at almost the same equilibrium distance *R*. As a result, the vibrational levels that are close in energy, i.e., roughly $O_2^+(A\,^2\Pi_u, v^+=0)$ and $O_2^+(a\,^4\Pi_u,\ v^+=10$ and above), feature highly oscillating wave functions of the quartet state that have very small overlap with those of the doublet state. On the contrary, vibrational levels of the $O_2^+(^2\Sigma_u^+)$ state are centered at a much larger equilibrium distance *R* and the overlaps of these levels with those of both $O_2^+(A\,^2\Pi_u)$ and $O_2^+(a\,^4\Pi_u)$ are relatively large, leading to larger shifts of about 1–10 cm^{-1} in A_{v+}. Two nearly degenerate vibrational levels of $O_2^+(A\,^2\Pi_u)$ and $O_2^+(^2\Sigma_u^+)$ combined with large vibrational interactions, are responsible for producing a large jump in A_{v+} at O_2^+ $(A\,^2\Pi_u,\ v^+=10)$, as can be seen on Fig 6. The A_{v+} value of 11.6 cm^{-1} for O_2^+ $(A^2\Pi_u,\ v^+=10)$, calculated incorporating the coupling between vibrational levels, is significantly higher than those for the adjacent O_2^+ $(A\,^2\Pi_u,\ v^+=9$ and 11) states. This result predicts that the strongest vibrational contribution for $O_2^+(^2\Sigma_u^+)$ occurs at O_2^+ $(A\,^2\Pi_u,\ v^+=10)$. Since no measurements for A_{v+} exist for O_2^+ $(A^2\Pi_u,\ v^+=9$ and 10), this theoretical prediction cannot be confirmed experimentally. Nevertheless, the previous experimental studies[5,10] suggest that the strongest vibrational interaction with $O_2^+(^2\Sigma_u^+)$ occurs at O_2^+ $(A\,^2\Pi_u,\ v^+=9$ and 10). This can be considered to be in reasonable agreement with the theoretical prediction at O_2^+ $(A\,^2\Pi_u,\ v^+=10)$ obtained in the present study.

As shown in Fig. 7, oscillations are observed in the $v^+=8-18$ range in the experimental A_{v+} curve[10] for $O_2^+(a\,^4\Pi_u)$. These oscillations may be due to vibrational interactions with other electronic states. The vibrational model predicts oscillations at $v^+>18$ with significantly lower amplitudes. Theoretically, the strongest coupling with other curves, mainly the $O_2^+(^2\Sigma_u^+)$ state, is seen at $v^+=21$ as compared to the experimental observation at $v^+=12$.

In the above model, the $O_2^+(a\,^4\Pi_u)$ state by itself has no influence upon the A_{v+} values of $O_2^+(A\,^2\Pi_u)$, owing to the fact that the perturbation causes both $O_2^+(A\,^2\Pi_{1/2u})$ and $O_2^+(A\,^2\Pi_{3/2u})$ components to be shifted by the same amount. The A_{v+} values of $O_2^+(a\,^4\Pi_u)$ can, however, be affected by interaction with the $O_2^+(A\,^2\Pi_u)$ state, i.e., the shifts of the levels belonging to a given spin-orbit multiplet for $O_2^+(a\,^4\Pi_u)$ are unequal. Nevertheless, the differences of these shifts are small and were not resolved in experimental[10] measurements. For this reason, only the average A_{v+} values obtained in the present theoretical studies are compared to experimental A_{v+} values. On the basis of the above analysis, we conclude that the observed fine features in the experimental A_{v+} curves shown in Figs. 6 and 7 cannot be attributed to spin-orbit coupling between $O_2^+(A\,^2\Pi_u)$ and $O_2^+(a\,^4\Pi_u)$ states. As noted in the previous paragraph, evidence exists that these fine structures, at least in part, arise from vibrational interactions with the $O_2^+(^2\Sigma_u^+)$ state. Other neglected interactions may play a role, of which derivative coupling between $O_2^+(X\,^2\Pi_g)$ and $O_2^+(A\,^2\Pi_u)$ is particularly worth mentioning.

IV. CONCLUSIONS

We have investigated the spin-orbit interactions of the $O_2^+(A\,^2\Pi_u)$, $O_2^+(a\,^4\Pi_u)$, and $O_2^+(^2\Sigma_u^+)$ states. The theoretical A_{v+} values for $O_2^+(A\,^2\Pi_u)$ and $O_2^+(a\,^4\Pi_u)$ calculated at the CASSCF and SOCI level of theory are in good quantitative agreement with experimental measurements. The truncated SOCI method does not perform decisively better than CASSCF, and in some ranges of v^+ SOCI actually gives worse agreement with experiment than CASSCF. The present theoretical study correctly predicts the inverted and regular nature of the spin-orbit splitting for $O_2^+(A\,^2\Pi_u)$ at low v^+ and high v^+ levels, respectively, observed in experimental studies. On the basis of the multistate vibrational interaction model, the strongest perturbation of $O_2^+(a\,^4\Pi_u)$ by $O_2^+(^2\Sigma_u^+)$ is predicted to occur at $v^+=10$, This is also consistent with the experimental finding at $v^+=9$ and 10. However, the multistate vibrational interaction calculations were unable to reproduce fine structures observed in the A_{v+} curves for $O_2^+(a\,^4\Pi_u)$, although there is evidence to explain them as a result of perturbation by the $O_2^+(^2\Sigma_u^+)$ state.

ACKNOWLEDGMENTS

This work was supported by the Director, Office of Energy Research, Office of Basic Energy Sciences, Chemical Science Division of the U. S. Department of Energy under contract No. W-7405-Eng-82 for the Ames Laboratory, and Contract No. DE-AC03-76SF00098 for the Lawrence Berkeley National Laboratory. Two of the authors (C.Y.N. and M.S.G.) acknowledge partial support from AFOSR. The authors also thank Professor C. Marian for very useful discussions. One of the authors (D.G.F.) acknowledges financial support from JSPS.

[1] D. S. Stevens, Phys. Rev. **38**, 1292 (1931).
[2] R. S. Mulliken and D. S. Stevens, Phys. Rev. **44**, 720 (1933).
[3] L. Bozoky, Z. Phys. **104**, 275 (1937).
[4] D. L. Albritton, W. J. Harrop, A. L. Schmeltekopf, and R. N. Zare, J. Mol. Spectrosc. **46**, 89 (1973).
[5] J. A. Coxon and M. P. Haley, J. Mol. Spectrosc. **108**, 119 (1984).
[6] J. Raftery and W. G. Richards, J. Chem. Phys. **62**, 3184 (1975).
[7] N. H. F. Beebe, E. W. Thulstrup, and A. Andersen, J. Chem. Phys. **64**, 2080 (1976).
[8] C. M. Marian, R. Marian, S. D. Peyerimhoff, B. A. Hess, R. J. Buenker, and G. Seger, Mol. Phys. **46**, 779 (1982).
[9] Y. Song, M. Evans, C. Y. Ng, C.-W. Hsu, and G. K. Jarvis, J. Chem. Phys. **111**, 1905 (1999).
[10] Y. Song, M. Evans, C. Y. Ng, C.-W. Hsu, and G. K. Jarvis, J. Chem. Phys. **112**, 1306 (2000).
[11] D. Fedorov, M. Evans, Y. Song, M. Gordon, and C. Y. Ng, J. Chem. Phys. **111**, 6413 (1999).
[12] Y. Song, M. Evans, C. Y. Ng, C.-W. Hsu, and G. K. Jarvis, J. Chem. Phys. **112**, 1271 (2000).
[13] M. W. Schmidt, K. K. Baldridge, J. A. Boatz *et al.*, J. Comput. Chem. **14**, 1347 (1993).
[14] MOLPRO is a package of *ab initio* programs written by H.-J. Werner and P. J. Knowles, with contributions from J. Almlöf, R. D. Amos, M. J. O. Deegan, S. T. Elbert, C. Hampel, W. Meyer, K. Meyer, K. Peterson, R. Pitzer, A. J. Stone, P. R. Taylor, and R. Lindh.
[15] H.-J. Werner and P. J. Knowles, J. Chem. Phys. **82**, 5053 (1985).
[16] P. J. Knowles and H.-J. Werner, Chem. Phys. Lett. **115**, 259 (1985).
[17] H.-J. Werner and P. J. Knowles, J. Chem. Phys. **89**, 5803 (1988).
[18] P. J. Knowles and H.-J. Werner, Chem. Phys. Lett. **145**, 514 (1988).
[19] M. W. Schmidt and M. S. Gordon, Annu. Rev. Phys. Chem. **49**, 233 (1998).
[20] H. A. Bethe and E. E. Salpeter, *Quantum Mechanics of the One and Two Electron Atoms* (Plenum, New York, 1977).
[21] D. G. Fedorov, Ph.D. thesis, ISU, 1999.
[22] K. P. Huber and G. Herzberg, *Molecular Spectra and Molecular Structure, Constants of Diatomic Molecules*, vol. IV (Van Nostrand, New York, 1979).
[23] *Modern Electronic Structure Theory, Part I*, edited by David R. Yarkony (World Scientific, NJ, 1995), specifically, p. 238.
[24] P. C. Cosby, J.-B. Ozenne, J. T. Moseley, and D. L. Albritton, J. Mol. Spectrosc. **79**, 203 (1980).
[25] J. C. Hansen, J. T. Moseley, and P. C. Cosby, J. Mol. Spectrosc. **173**, 48 (1983).